Vol. 42, No. 4 (2020) 582-591, DOI: 10.24874/ti.855.02.20.10

Tribology in Industry

www.tribology.rs

RESEARCH

Hardness and Wear Behavior of Al 6061/ZrC Composite Processed by Friction Stir Processing

T.S. Kumar[a,*], R. Raghu[b], S. Shalini[c]

[a]*Department of Mechanical Engineering, Amrita School of Engineering, Coimbatore, Amrita Vishwa Vidyapeetham, India,*
[b]*Department* of *Mechanical Engineering, Sri Ramakrishna Engineering College, Coimbatore-641022, Tamilnadu India,*
[c]*Department of Physics, PSG Polytechnic College, Coimbatore-641004, Tamilnadu, India.*

Keywords:

Al6061/ZrC composite
Friction Stir Processing
Hardness
Sliding wear

* Corresponding author:

T. Satish Kumar
E-mail: t_satishkumar@c.amrita.edu

Received: 29 February 2020
Revised: 30 April 2020
Accepted: 6 October 2020

A B S T R A C T

Friction Stir Process (FSP) was handled to produce Al6061/ZrC composite. Three different groove widths were produced to reinforce three different ZrC volume fractions (3, 6 and 9 %) in the matrix. Processing of the composite was carried out at Tool Rotational Speed of 1200 rpm and traverse speed of 30 mm/min. Microhardness test of the composites was conducted through microhardness tester. Sliding wear behavior of the composite was investigated using the pin-on-disc tribometer and the worn-out surfaces were examined to observe the wear mechanisms. Results showed that microhardness has enhanced with the addition of ZrC particles upon grain refinement, uniform dispersion, and greater bonding. The wear resistance has increased with the increase in the volume fraction of the reinforcement particles. The worn-out surface showed that wear transitioned from severe to mild type as the volume fraction of reinforcement increases.

1. INTRODUCTION

Aluminium alloys are utilized in automobile, aerospace and marine applications owing to its lightweight. Specifically, Al6061 aluminium alloy has been used for the production of aircraft components. However, its extensive usage is limited due to inferior tribological behaviour [1]. Particle reinforced aluminium composites are emerging as the potential alternative materials for the aluminium alloys owing to its greater tribological properties. Various researchers reported that SiC and Al_2O_3 are the often incorporated reinforcement for the enhancement of mechanical and wear properties of Al6061 alloys [2-3]. Several processing routes under liquid and solid-state are used for fabrication of such Metal Matrix Composites (MMCs) [4-6].

Aluminium 6061/graphene composites were manufactured through powder metallurgy route and its flexural strength was assessed to compare its performance with unreinforced alloy. Results revealed that the flexural strength of the composite was 47 % more than that of unreinforced alloy [7].

Investigation on wear behaviour of the Al6061/Carbon Nano Tube (CNT) Reinforced

composites (0.5-2 wt%) fabricated through Spark Plasma Sintering (SPS) technique was carried out. It is stated that Al6061 alloy reinforced with 1 wt% CNT exhibited a lower coefficient of friction (0.35) and better wear resistance [8]. Wear behaviour of Al6061 alloy reinforced with a different fraction of graphite (5, 10 and 15 wt%) through the casting process has been investigated. Results showed that 5 wt% reinforced composite resulted in greater wear resistance than that of the unreinforced alloy owing to its self-lubrication characteristics [9].

Recently emerged solid-state processing technique to enhance the wear resistance of the composites is the Friction Stir Processing (FSP). This process offers homogenous dispersion of reinforcement as well as microstructure modification [10,11]. In addition to microstructural modification, this technique is an effective method for processing of MMCs [12,13]. In this process, a tool is rotated and simultaneously inserted into the surface of the material followed by a transverse feed of the tool in the material [14]. The rotational motion of the tool induces stirring of the reinforcement in the metal surface and generates heat due to friction between the metallic surface and the tool. These action consequences in the incorporation and homogeneous distribution of the reinforcements in the matrix.

Al6061 alloy was reinforced with SiC particles (20 μm) through the FSP process and observed uniform dispersion of SiC particles in the matrix. Al6061-SiC-Graphite hybrid composite processed at a traverse speed of 60 mm/min with 900, 1120 and 1400 rpm has been done. It is stated that composite processed at a slower rotational speed (900 rpm) exhibited a lower wear rate of 2 mm^3/m in contrast to the composite (6 mm^3/m) processed at 1400 rpm. Wear rate of the FSPed 6061/ Al_2O_3-graphite hybrid composite processed at a traverse speed of 60 mm/min and 700 rpm is measured. It is observed that the composite attained higher hardness of 165 BHN and lower wear rate of 0.812 g/s when compared to the unreinforced alloy due to grain refinement up to 10 μm [15].

Numerous researchers investigated on the incorporation of constant wt% of reinforcement in the alloy through FSP and studied their properties. Besides, wear behaviour of ZrC reinforced Al6061 composite processed through FSP has not been focused. Therefore the present study concentrates on FSP of Al6061/ZrC composite to study the effect of different fraction of ZrC on its microstructure characteristics, mechanical properties and sliding wear behaviour.

2. MATERIALS AND METHODS

Al6061 alloy (composition in wt%: 0.8 Si, 0.7 Fe, 0.4Cu, 0.8 Mg, 0.25 Zn and balance Al) is taken in the form of plates with the dimensions of 5 × 10 × 0.5 cm. The groove is taken along the length of the sample in the center axis of width on the surface. The groove dimension (groove width and groove depth) is varied to obtain a varied volume fraction of the reinforcement in the composite i.e 3, 6 and 9 % volume ZrC. Figure.1 shows the SEM image of the ZrC particles and its XRD pattern. ZrC paricles with average size of 1-5 μm was used in the present study. The formula used to calculate the volume fraction of the reinforcement along with the calculations is given in Table 1.

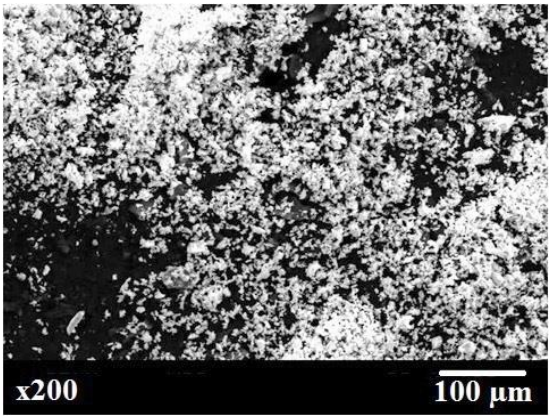

a)

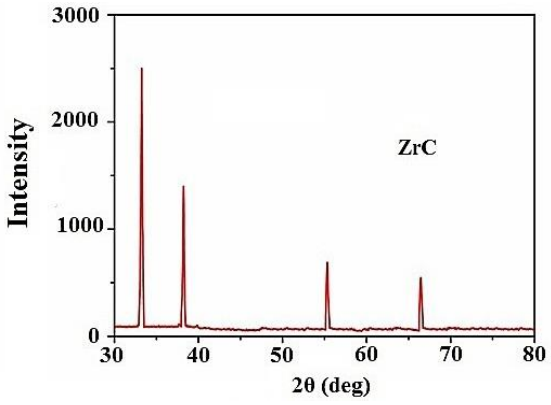

b)

Fig. 1. (a) SEM image of the ZrC particles and (b) XRD pattern of ZrC particles.

Table 1. Calculation of volume fraction of reinforcement particles.

Sample No.	Groove Width (mm)	Groove Depth (mm)	Groove Area (Sq.mm)	Theoretical Volume fraction of reinforcement particles [(V_t) = (Groove area/Projected area of tool pin)*100]
1	1.3	1	1.3	~ 3
2	1.8	1.5	2.7	~ 6
3	2	2	4	~ 9

The axial load of 6 kN, a rotating speed of 1200 rpm and traverse speed of 30 mm/min is employed to perform the process The angle of the pin is kept at 2° and it is embedded 4 mm deep into the sample during FSP. To manage consistent distribution of the ZrC particles, initially groove is made on the surface of the specimen and it has been filled with ZrC particles. To prevent scattering of particles during FSP, pinless tool is made to traverse along the surface of the specimen. This action of pinless tool seals the groove and compresses the particles in the groove so that no loss in reinforced particles occurs. Then a tool with a pin at its end with dimensions ᵠ8mm*5mm is used to fabricate the composite. This action of tool causes intense stirring, high plastic strain and sufficient material flow which aids in consistent distribution of the ZrC particles. FSPed Al 6061 alloy composite specimens were polished using different grades of emery sheets (320, 1000, 1500 and 2000) until a surface with minimum scratches is obtained. Then the specimens are disc polished until a mirror finish is obtained. The polished specimens were examined through a Scanning Electron Microscope (SEM) to observe the distribution of ZrC particles in the matrix alloy.

Hardness test was carried on different zones in the FSPed composite to study the variation of hardness in the composite as per ASTM E 384. The specimen was subjected to a load of 100g and the indentation is brought by a diamond pyramid indenter. Hardness is expressed in Vickers Pyramid Number (HV). The composite specimens were subjected to pin-on-disc wear test (as per ASTM G99) experiments designed using the Box Behnken design method (Table 2). Three parameters are considered such as volume fraction of the reinforcement particles, sliding velocity and the load. The tests are carried out at room temperature with a constant sliding distance of 1000 m and sliding radius of 50 mm. The weight of the sample before each experiment is measured and after each run, the weight loss due to wear is measured in a digital weighing scale. The wear rate and specific wear rate of each sample are also calculated.

Table 2. Experimental design as per the Box-Behnken Method.

Trial No	% ZrC	Sliding Velocity, S (m/s)	Load, P (N)
1	9	2	10
2	3	2	30
3	6	2	30
4	9	2	30
5	3	2	10
6	6	2	20
7	3	3	20
8	6	3	10
9	9	3	20
10	3	1	20
11	6	2	10
12	9	1	20
13	6	1	10
14	6	1	30
15	6	3	30

3. RESULTS AND DISCUSSION

3.1. SEM analysis

FSPed specimens are examined through SEM with EDS and the obtained microstructures with spectrum are displayed in Fig. 2. Microstructures revealed the presence of the reinforced ZrC particles in the matrix which shows that reinforced particles possess uniform dispersion in the matrix. It is also observed that as the volume fraction of the reinforcement particles in the matrix increases, the particles tend to occur individually rather than in clusters. This evident that even at a high volume fraction of ZrC particles (9 %), homogeneous distribution has resulted without agglomeration of the ZrC particles. There is a decrement in particle size when the volume fraction of the reinforcement has increased. The variation in the volume fraction of ZrC particles is seen in Fig. 2.

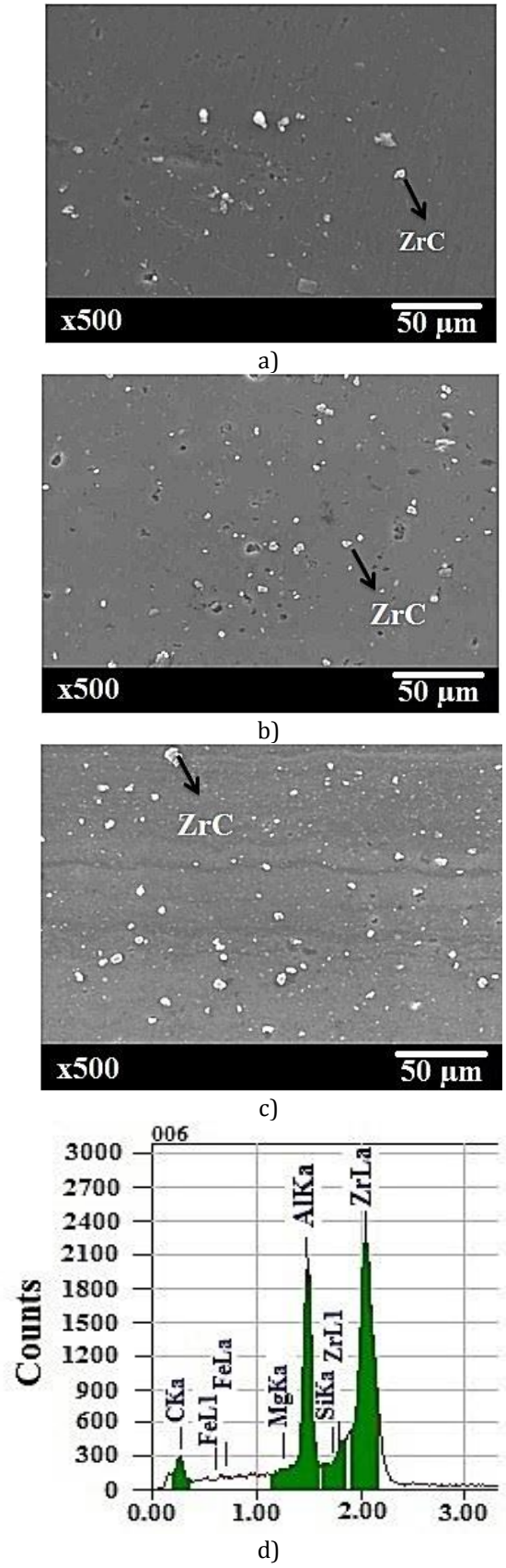

Fig. 2. SEM images of Al 6061 samples FSPed with (a) 3 % Volume ZrC particles, (b) 6 % Volume ZrC particles, (c) 9 % Volume ZrC particles in the stir zone and (d) EDS spectra of 9 % Volume ZrC reinforced composite.

3.2 Hardness survey

The hardness survey taken across the composite surface in the direction normal to that of the feed direction is shown in Fig. 3. When compared to the base material (Al6061) hardness (49 HV), there is a notable increase in hardness as the volume fraction of the reinforcement particles increases. This is attributed to the Orowan's strengthening which is prime in the FSPed composites.

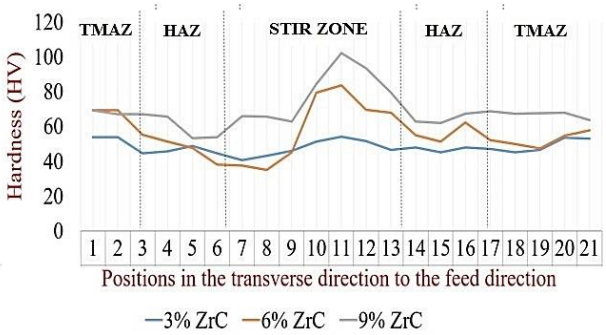

Fig.3. Hardness survey plot (with data) for Al 6061 composite sample with a varied volume fraction of ZrC reinforcement.

The reinforcement particles in the stirring zone obstruct the dislocation movement while deformation process and consequences in an increase in dislocation density in the matrix. The volume fraction of ZrC increases as there is an increase in groove width which resulted in a higher number of dislocations along with less interparticle spacing. This in turn produces the interaction of the dislocation with the ZrC and higher hardness of the composite. It is observed that hardness is greater in the stir zone compared to the TMAZ and HAZ zone. The hardness is either the same or less than that of the base material in the HAZ, depicting that the HAZ in all the three composite samples is the weaker zone. However, there is increase in the hardness of HAZ with respect to increase in the reinforcement volume fraction. This is attributed to increase in the dislocation density in HAZ with increase in the reinforcement. The HAZ, although inevitable, can be minimized further by optimizing the friction stir processing parameters. This, however, could be taken as the scope for future studies. As a whole, it is observed that hardness increase in the stir zone is due to i) grain growth prevention by ZrC reinforcement particles and grain refinement at the stir zone ii) uniform dispersion of

reinforcement particles owing to the proper material flow in the stir zone, and iii) greater bonding of 6061 with the ZrC particles.

3.3 Dry sliding wear test

The wear tests were carried out as per ASTM G99 using the DOE by Box Behnken method. Wear rate (Eqn. 1) for each sample is calculated as the volume of material lost per unit sliding distance.

$$W = \Delta V/d \quad (1)$$

Where ΔV is the volume loss in m^3 and d is the sliding distance in m. Simply wear rate does not include the influence of the applied load. Hence, the specific wear rate for each experiment is calculated as per Eqn. 2 [16,17] and shown in Table 3.

$$W = \Delta V/Ld \quad (2)$$

Where ΔV is the volume loss in mm^3, L is the load in Newton, and d is the sliding distance in m. The results were analyzed using the Minitab software and the contour plots are also extracted to know the effect of the variables on the wear rate of the composite. The contour plot for the variation of wear rate to variation in sliding velocity and volume fraction of ZrC particles at a constant load of 10 N is shown in Fig. 4.

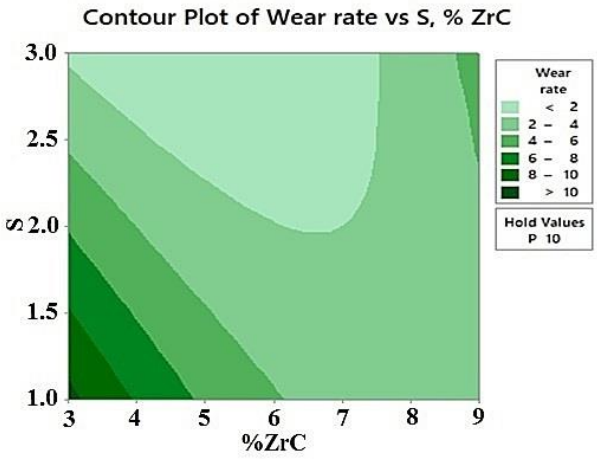

Fig. 4. Effect of sliding velocity and volume fraction on wear rate at a load of 10 N.

From the contour plot (Fig. 4), at low volume fraction (3 %) and low sliding velocity of 1 m/s, the wear rate is found higher. This is due to the presence of less number of reinforcement particles at the surface which is not adequate in providing better wear resistance at low sliding velocity. It is known that hardness is linearly related to the wear resistance. The low volume fraction of reinforcement imparted less hardness to the surface hence high wear rate has resulted under such condition.

Table 3. Wear rate and specific wear rate for the FSPed 6061/ZrC composite specimens.

Expt No	%ZrC	Sliding Velocity, S (m/s)	Load, P (N)	Wear Rate (m^3/m sliding distance))× 10^{-13}	Specific Wear Rate (m^3/N-m))× 10^{-14}
1	9	2	10	5.185	5.185
2	3	2	30	7.037	2.3456
3	6	2	30	8.518	2.839
4	9	2	30	0.3703	0.123
5	3	2	10	6.290	6.296
6	6	2	20	3.333	1.666
7	3	3	20	3.333	1.666
8	6	3	10	1.481	1.481
9	9	3	20	2.592	1.296
10	3	1	20	15.18	7.59
11	6	2	10	0.3703	0.3703
12	9	1	20	4.074	2.037
13	6	1	10	1.975	1.975
14	6	1	30	3.765	1.255
15	6	3	30	0.4507	0.1502

The mechanism behind the high wear rate at low sliding velocity (1 m/s) is due to the increased amount of contact time of the specimen with the counterface. Usually at low velocity, the time taken to cover the sliding distance of 1000 m would be higher which eventually results in higher metallic contact and higher wear rate compared to higher velocities. However for low sliding velocity, as the volume fraction of reinforcement is increased, the wear rate is found decreased. The increase in volume fraction increased the wear resistance of the FSPed composite due to the higher hardness imparted by high volume fraction of reinforcement even at low sliding velocity. Besides, greater bonding and uniform dispersion of the reinforcement particles with the matrix aided in greater wear resistance. The high volume fraction of reinforcement particles in the surface reduces the direct contact of the matrix surface with the counterface. Hence, it evident that incorporation of high volume fraction of ZrC particles in the aluminium enhanced the wear resistance of the FSPed composite at all sliding velocities.

The decrease in wear rate as the sliding velocity (3 m/s) increases for different volume fraction of reinforcement is attributed to the temperature increase at the interface of composite and counterface. This temperature increase, in turn, forms a protective layer on the specimen surface due to transfer of materials which consequences in the prevention of wear during sliding. However at higher sliding velocity of 3 m/s and higher volume fraction of 9 %, there is again a slight increase in wear rate. At this higher volume fraction, more fraction of materials transfer takes place which is difficult to be accommodated in the contact interface. This eventually tends to deteriorate a part of the protective layer and consequences in slight increase in wear rate.

The contour plot for the variation of wear rate to variation in sliding velocity and volume fraction of ZrC particles at a constant load of 20 N is shown in Fig. 5.

The similar trend in wear rate is observed with variation in sliding velocity and volume fraction in case of 20 N load. Similar pattern of slight increase in wear rate is observed at high velocity and high volume fraction condition for the applied load of 20 N. This is assumed due to the slight deterioration of the protective layer formed over the surface as likely in case of 10 N.

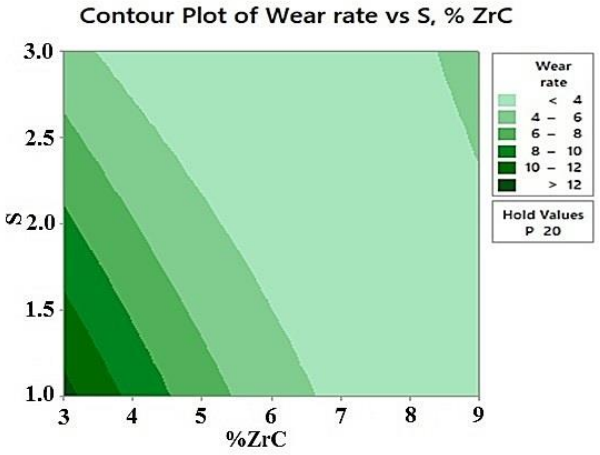

Fig. 5. Effect of sliding velocity and volume fraction on wear rate at a load of 20 N.

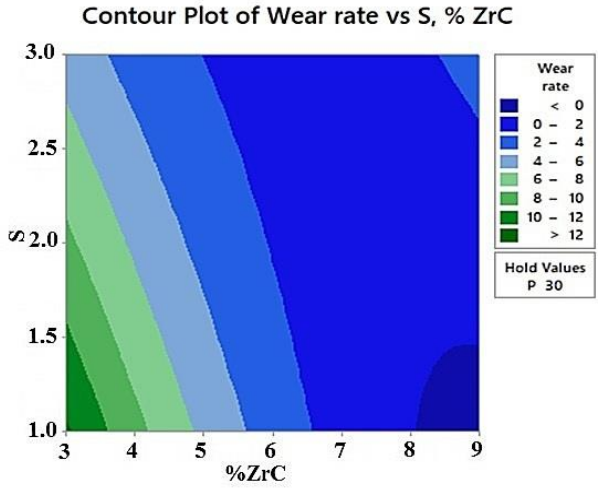

Fig.6. Effect of sliding velocity and volume fraction on wear rate at a load of 30 N.

The increase in the magnitude of the wear rate is observed in 20 N load when compared to the contour plot at a load of 10 N. This plot shows that variation in load has a greater influence on the variation of the wear rate. It is inferred that an increase in external load deforms the specimen surface upon continuous sliding contact with the counterface. At low load condition, the pressure and deformation of the specimen will be at a minimum level which consequences in less amount of material removal. The increase in load generally increases the specimen contact with the rotating counterface which in turn increases the wear rate. This in turn increases the interfacial pressure and results in more deformation as well as material removal.

The contour plot for the variation of wear rate to variation in sliding velocity and volume fraction of ZrC particles at a constant load of 30 N is shown in Fig. 6.

From this contour plot (Fig. 6), it is observed that the wear rate is higher at low velocity and low volume fraction of reinforcement. The wear rate gets decreases as the velocity increases for all fractions of reinforcement. Similarly, the wear rate decreases as the volume fraction increase for all levels of sliding velocities. Overall, it is inferred that the wear rate gets decreased with an increase in sliding velocity and volume fraction. However, the similar nature of deterioration of protective layer and slight increase in wear rate is found in case of high sliding velocity and high volume fraction at load of 30 N as likely in case of 10 N and 20 N. As the velocity and volume fraction increases, the wear rate found decreasing as like in case of 10 N and 20 N. However the magnitude of wear rate is further increased in a load of 30 N when compared to the lower loads of 10 and 20 N.

3.4 Optimization of the parameters

Optimization of the response is carried out in the Box-Behnken analysis to identify the combination of the parametric condition which aids in attaining desired wear rate by determining the relation of the wear rate with the parameters such as load, velocity and volume fraction. The target and the upper wear rate were given as input in the optimization process and the optimum parametric condition resulted is displayed in the optimization plot (Fig. 7). The global solution to attain a wear rate of 0.378 m^3/m is a volume fraction of 8.8 % ZrC, sliding velocity of 1.049 m/s and a load of 28 N.

3.5 SEM analysis

The samples obtained after the dry sliding wear test were examined through SEM to address the wear mechanism. Figure 8 shows the wear mechanisms of the composite samples reinforced with 3 % ZrC particles tested at different sliding velocities and different load condition. From Figure 8a, it is observed that surface under high loading condition (30 N) experienced greater deformation due to the high physical pressure at the interface. The worn-out surface revealed the deformation with surface delamination and removal of material. This evidence that the wear has transitioned from mild to a severe condition as the load is increased on the low fraction reinforced surface (3 %). On the other hand, surface (Fig. 8b) subjected to low load (10 N) is observed with less number of grooves and scratches owing to low pressure at the interface. In Figure 8c, the surface tested under the velocity of 3 m/s revealed the uniform wear on the surface along with micro-ploughing. The transition of the wear mechanism of the composite specimen from a velocity of 1 to 3 m/s shows that there is less deformation due to the less contact time established at high velocity. The surface (Figure 8d) subjected to low velocity (1 m/s) condition showed deeper wear track abruptly. The more amount of material removal is reasoned to the high contact time of the counterface with the specimen which facilitated adequate contact of the total area at the interface.

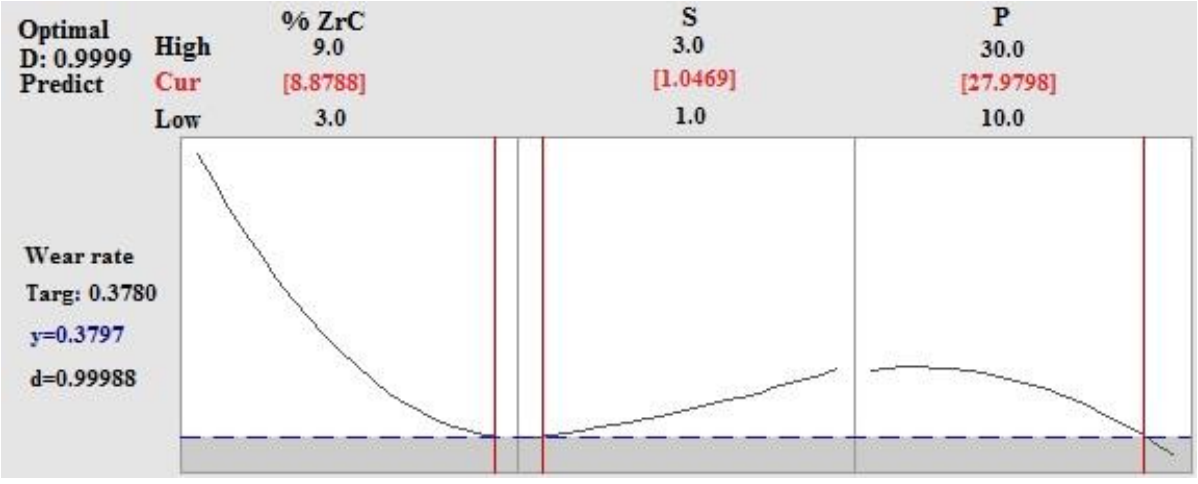

Fig. 7. Optimization plot for a desired wear rate of 0.378m^3/m.

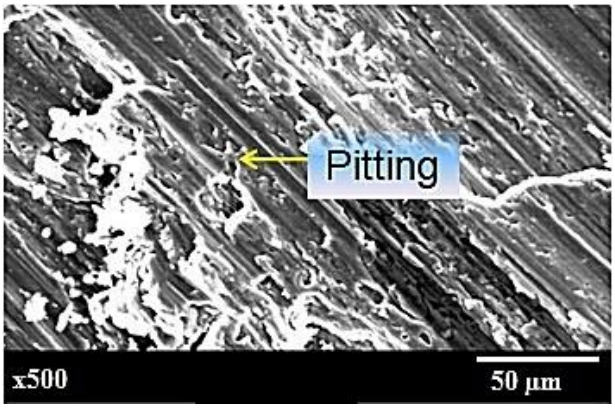

a)

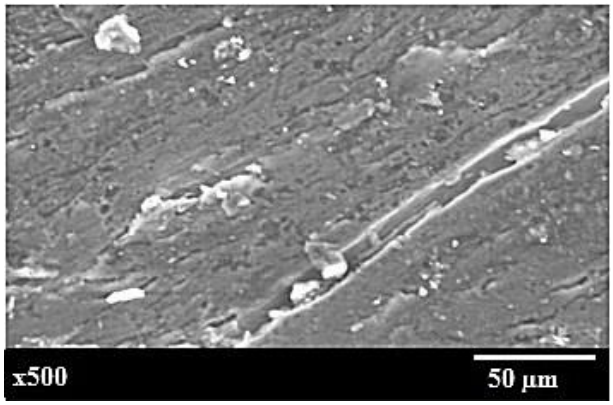

b)

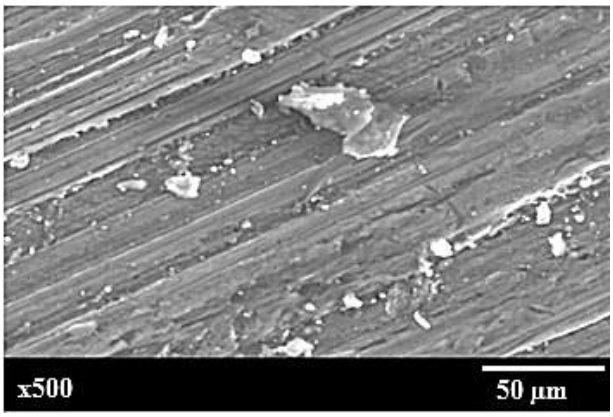

c)

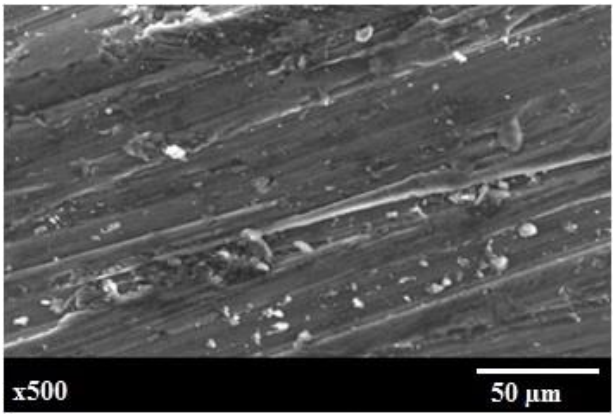

d)

Fig. 8. SEM micrographs of the composite samples with 3% ZrC particles (a) 2 m/s and 30 N (b) 2 m/s and 10 N (c) 3 m/s and 20 N (d) 1 m/s and 20 N.

The SEM micrograph of the composites with 9 % ZrC particles is shown in Fig. 9. The wear mechanism was turned mild at all conditions for the composite specimens with 9 % ZrC particles compared to 3 % ZrC particles. The worn-out surface (Fig. 9a) at low load (10 N) shows mild wear and the surface (Fig. 9b) at high load (30 N) shows the transition of mild wear to a slightly increased amount of material removal.

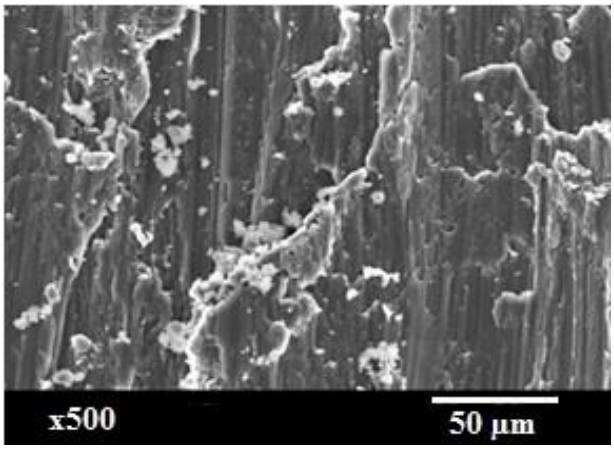

a)

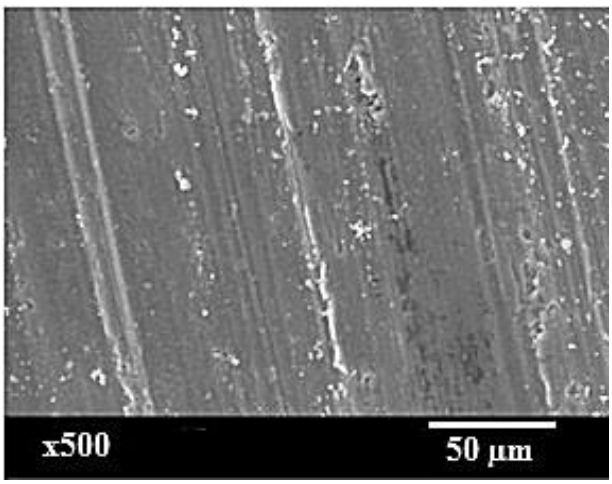

b)

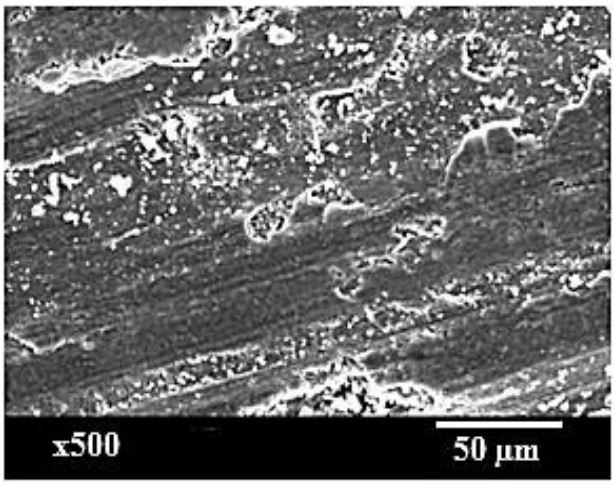

c)

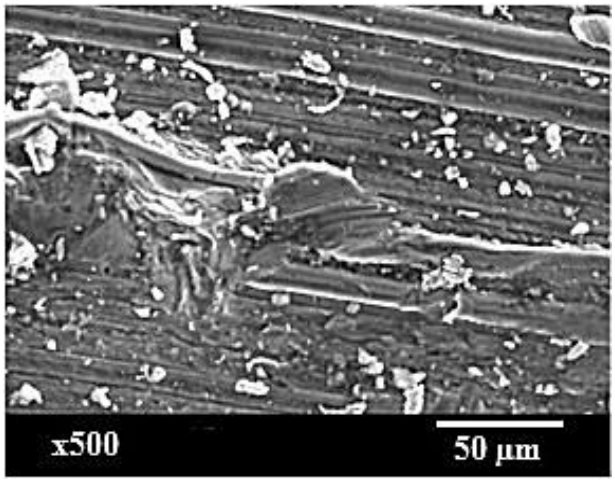

d)

Fig. 9. SEM micrograph of the composite samples with 9 % ZrC particles (a) 2 m/s and 30 N, (b) 2 m/s and 10 N, (c) 3 m/s and 20 N and (d) 1 m/s and 20 N.

As the wear gets transitioned with an increase in load, the high volume fraction of ZrC particles at the surface delays the transition of wear. This evident that 9 % of ZrC particles reinforced composites exhibited greater wear resistance over the 3 % and 6 % ZrC particles reinforced composite even at high load condition (30N). This is attributed to the underlying Orowan dispersion strengthening mechanism offered by ZrC particles predominant in case of composites. These particles act as the obstacles towards the movement of dislocation as the material deforms. Therefore these dislocations bend and form a loop around the ZrC particles and move forward. This action of dislocation tends to form continuous loops over the particles which in turn produces back stress and restricts the movement of further dislocations. Thus higher stress is required for slip process to happen which consequences in the strengthening of the composites. The required stress for further slip process is inversely proportional to the distance between the ZrC reinforcement particles. Thus the particle with higher volume fraction i.e., 9 % will have less interparticle distance and exhibits greater wear resistance at all conditions.

At increased velocity (Fig. 9c) the surface shows less amount of pitting and the wear is more uniform. At lower sliding velocity (Fig. 9d), the particles cause the turbulence like nature in the worn path due to sufficient contact of the specimen and the counterface.

4. CONCLUSION

Fabrication of Al6061 composite reinforced with ZrC particles is done successfully done using Friction stir processing. Hardness (HRc) measurements show that, with an increase in a volume fraction of ZrC particles the hardness increases in the stir zone. However, the softening of HAZ is inevitable. SEM analysis reveals the distribution of ZrC particles in the matrix and also they are effectively bonded in the matrix. Wear rate decreases with an increase in sliding velocity and increase in volume fraction of the reinforcement particles whereas the wear rate increases with increase in applied load.

REFERENCES

[1] D. Aruri, K. Adepu, K. Adepu, K. Bazavada, *Wear and mechanical properties of 6061-T6 aluminum alloy surface hybrid composites [(SiC+Gr) and (SiC+Al_2O_3)] fabricated by friction stir processing*, Journal of Materials Research and Technology, vol. 2, iss. 4, pp. 362-369, 2013, doi: 10.1016/j.jmrt.2013.10.004

[2] G.B.V. Kumar, C.S.P. Rao, N. Selvaraj, M.S. Bhagyashekar, *Studies on Al6061-SiC and Al7075-Al_2O_3 Metal Matrix Composites,* Journal of Minerals and Materials Characterization and Engineering, vol. 9, no. 1, pp. 43-55, 2010, doi: 10.4236/jmmce.2010.91004

[3] A. Devaraju, A. Kumar, A. Kumaraswamy, B. Kotiveerachari, *Influence of reinforcements (SiC and Al_2O_3) and rotational speed on wear and mechanical properties of aluminium alloy 6061-T6 based surface hybrid composites produced via friction stir processing*, Materials and Design, vol. 51, pp. 331-341, 2013, doi: 10.1016/j.matdes.2013.04.029

[4] S.K. Thandalam, S. Ramanathan, S. Sundarrajan, *Synthesis, Microstructural and Mechanical Properties of Ex-Situ Zircon Particles ($ZrSiO_4$) Reinforced Metal Matrix Composites (MMCs): A Review,* Journal of Material Research and Technology, vol. 4, iss. 3, pp. 333-347, 2015, doi: 10.1016/j.jmrt.2015.03.003

[5] N. Radhika, *Analysis of Tribological Behaviour of Functionally Graded LM13 Aluminium/TiS_2 Composite Using Design of Experiments*, Tribology in Industry, vol. 38, no. 3, pp. 425-434, 2016.

[6] N. Radhika, R. Raghu, *Evaluation of Dry Sliding Wear Characteristics of LM 13 Al/B_4C Composites*, Tribology in Industry, vol. 37, no. 1, pp. 20-28, 2015.

[7] M. Bastwros, G.-Y. Kim, C. Zhu, K. Zhang, S. Wang, X. Tang, *Effect of ball milling on graphene reinforced Al6061 composite fabricated by semi-solid sintering*, Composites Part B: Engineering, vol. 60, pp. 111-118, 2014, doi: 10.1016/j.compositesb.2013.12.043

[8] A.M. Al-Qutub, A. Khalil, N. Saheb, A.S. Hakeem, *Wear and friction behavior of Al6061 alloy reinforced with carbon nanotubes*, Wear, vol. 297, iss. 1-2, pp. 752-761, 2013, doi: 10.1016/j.wear.2012.10.006

[9] A. Baradeswaran, A. Elayaperumal, *Wear characteristics of Al6061 reinforced with graphite under different loads and speeds*, Advanced Materials Research, vol. 287-290, pp. 998-1002, 2011, doi: 10.4028/www.scientific.net/AMR.287-290.998

[10] A.J. Alex, R.V. Vignesh, R. Padmanaban, M. Govindaraju, *Effect of heat treatment on the mechanical and wear behavior of friction stir processed AA5052 alloy*, MaterialsToday: Proceedings, vol. 22, iss. 4, pp. 3340-3346, 2020, doi: 10.1016/j.matpr.2020.03.297

[11] T.S. Kumar, S. Shalini, K.K. Kumar, *Effect of friction stir processing and hybrid reinforcement on wear behaviour of AA6082 alloy composite*, Materials Research Express, vol. 7, no. 2, pp. 1-8, 2020, doi: 10.1088/2053-1591/ab6e2a

[12] Y.X. Gan, D. Solomon, M. Reinbolt, *Friction stir processing of particle reinforced composite materials*, Materials, vol. 3, iss. 1, pp. 329-350, 2010, doi: 10.3390/ma3010329

[13] S. Sahraeinejad, H. Izadi, M. Haghshenas, A.P. Gerlich, *Fabrication of metal matrix composites by friction stir processing with different Particles and processing parameters*, Material Science and Engineering: A, vol. 626, pp. 505-513, 2015, doi: 10.1016/j.msea.2014.12.077

[14] S.J. Singh Gurmeet, Goyal Navneet, Singh Kulwant, *Mathematical modeling of process parameters in friction stir welding of aluminium*, International Journal of Advanced Engineering Technology, vol. 1, no. 3, pp. 145-158, 2010.

[15] T. Prakash, S. Sivasankaran, P. Sivasankar, *Mechanical and Tribological Behaviour of Friction-Stir-Processed Al 6061 Aluminium Sheet Metal Reinforced with Al_2O_3/0.5 Gr Hybrid Surface Nanocomposite*, Arabian Journal for Science and Engineering, vol. 40, pp. 559-569, 2015, doi: 10.1007/s13369-014-1518-4

[16] M. Sudheer, R. Prabhu, K. Raju, T. Bhat, *Modeling and Analysis for Wear Performance in Dry Sliding of Epoxy/Glass/PTW Composites Using Full Factorial Techniques,* International Scholarly Research Notices, vol. 2013, pp. 1-11, 2013, doi: 10.5402/2013/624813

[17] S.A. Bello, J.O. Agunsoye, J.A. Adebisi, N.K. Raji, S.B. Hassan, *Wear resistance properties of epoxy aluminium microparticle composite*, Proceedings on Engineering Sciences, vol. 1, no.1, pp. 58-65, 2019, doi: 10.24874/PES01.01.007